CHAPTER 21

Euclidean Rhythms, Euclidean Strings, and Well-Formed Rhythms

In the year 300 BC, the city of Alexandria in present-day Egypt was endowed with a magnificent library similar in spirit to the modern institution we call a university. In this Royal Library, which contained reading rooms and a large quantity of books in the form of papyrus scrolls, scholars from diverse parts of the neighboring world, financially supported by the government in Alexandria, gathered together to carry out research and write about a wide variety of topics including astronomy, geometry, and music.[1] One scholar in particular, named Euclid, wrote a book that became one of the best sellers of all time for more than 2,000 years. This book, titled *The Elements*, contains a wonderful compilation of algorithms (recipes) that were known at that time for solving an extensive variety of *geometric* problems that many of us have studied in secondary school.[2] Aside from geometry, Euclid also described a compelling algorithm for solving a fundamental problem concerned with the arithmetic of *numbers*. This algorithm has found many mathematical and computational applications since then, and is still actively investigated today.[3] Little did Euclid know that 2,300 years later this numerical algorithm would be shown to generate traditional musical rhythms used throughout the world. Although some readers may be surprised to learn that numbers and music are intimately related, the German philosopher and mathematician Gottfried Leibniz wrote: "*The pleasure we obtain from music comes from counting, but counting unconsciously. Music is nothing but unconscious arithmetic.*"[4]

The algorithm in question is one of the oldest and well-known algorithms, described in Propositions 1 and 2 of *Book VII* of *The Elements*. Today it is referred to as the *Euclidean algorithm*. This algorithm solves the problem of computing the greatest common divisor of two given natural numbers. The computer scientist Donald Knuth calls it the "granddaddy of all algorithms, because it is the oldest nontrivial algorithm that has survived to the present day." The idea is captivatingly simple. Repeatedly, replace the larger of the two numbers by their difference until both are equal. This last number is then the greatest common divisor. Consider as an example the pair of numbers (3, 8). First, eight minus three equals five, so we obtain the new pair (3, 5); then, five minus three equals two giving (3, 2); next, three minus two equals one which yields (1, 2); and lastly two minus one equals one, which results in (1, 1). Therefore, the greatest common divisor of three and eight is one. This procedure admits a compelling visualization illustrated in Figure 21.1 for the pair of numbers (3, 8). First, construct a 3×8 rectangle of unit squares as shown in the upper left. Repeatedly subtract a 3×3 square from this rectangle until it is impossible to do so. This leaves a 2×3 rectangle remaining (upper right). Now proceed to remove 2×2 squares from this 2×3 rectangle until it cannot be done. This yields the 2×1 rectangle remaining (lower left). Finally, remove a 1×1 square from the 2×1 rectangle to obtain a 1×1 square remaining.

How do we make the Euclidean algorithm generate musical rhythms? The key is to shift our attention from the answer given by the algorithm to the

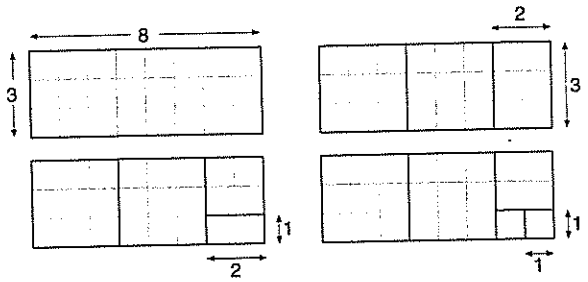

FIGURE 21.1 Visualization of the *Euclidean* algorithm for computing the greatest common divisor of integers 3 and 8 by repeated subtraction.

"history" (or sequence of calculations) of the algorithm, as it progresses towards the answer. This procedure is illustrated with the preceding pair of numbers (3, 8). For this purpose, the smaller number three is associated with the number of onsets that we want the rhythm to have, and the larger number eight, with the total number of pulses (onsets and silent pulses) that determine the rhythmic span or cycle. The algorithm illustrated in Figure 21.2 uses box notation. First write a rhythm of eight pulses and three onsets in which all the onsets are completely on the left at pulses 1, 2, and 3 as in Figure 21.2a. Next take (subtract) a number of silent pulses equal to the number of onsets (in this case three), from the right (pulses 6, 7, and 8) and place them below the others, flush to the left as in Figure 21.2b. Now there is a remainder of two silent pulses. Move these below the rest, also flush to the left, as in Figure 21.2c. Now that we have a single column remaining at pulse position three, the repeated subtraction phase of the algorithm is finished. The concatenation phase of the algorithm follows next. First separate the three columns as in Figure 21.2d. Next, rotate each column to become a row as in Figure 21.2e, and lastly, concatenate the three rows to form the generated rhythm in Figure 21.2f. Note that the rhythm generated by this procedure is none other than the [3-3-2] pattern found all over the world. In particular it is the Cuban *tresillo* as well as the first half of the *clave son*, which we have encountered repeatedly throughout the book.

This procedure attempts to distribute the three onsets among the eight pulses as evenly as possible. It is this property that, to a large extent, is most responsible for obtaining rhythms that are popular throughout the world. The rhythms generated in this way are called *Euclidean* rhythms, because they are generated using an implementation of the Euclidean algorithm, and will be denoted by E(k,n), where k is the number of onsets and n is the number of pulses in the cycle. Thus, the Cuban tresillo is denoted by E(3,8). Other than k being smaller than n, there are no restrictions on these values. Hence, Euclidean rhythms constitute a broader set of rhythms than the family of *diatonic* rhythms. Jesse Stewart defines a *diatonic* rhythm "as a repeating rhythmic pattern in which an odd number of sounded pulses are spread out as much as possible across the tones of an even-numbered time cycle (generally consisting of 8, 12, or 16 pulses)."[5] Therefore, except for $k = 3$, and $n = 12$, which yield the regular Euclidean rhythm with interval structure [3-3-3-3], all other diatonic rhythms with an odd value of k, and $n = 8$, 12, and 16, are irregular.

When the number of sounded pulses (onsets) is greater than the number of silent pulses, all the silent pulses are moved in the first step of the algorithm. The remainder of the procedure remains the same. This process is illustrated with the numbers (5, 8) in Figure 21.3. First, the three silent pulses (6, 7, 8) are moved, as in Figure 21.3b. Now there are two single-onset columns remaining at pulse positions 4 and 5. These are moved next, as in Figure 21.3c. The concatenation phase in Figure 21.3d–f is the same as before. Note that the resulting Euclidean rhythm E(5,8) is the Cuban cinquillo timeline [2-1-2-1-2].

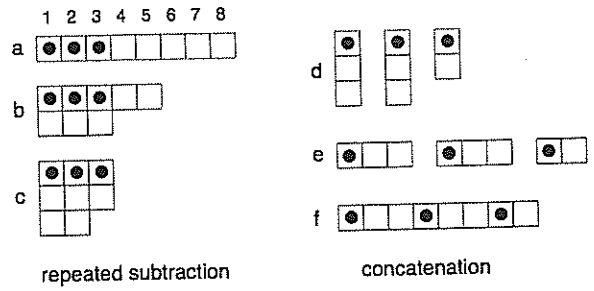

FIGURE 21.2 Generation of the Cuban *tresillo* timeline.

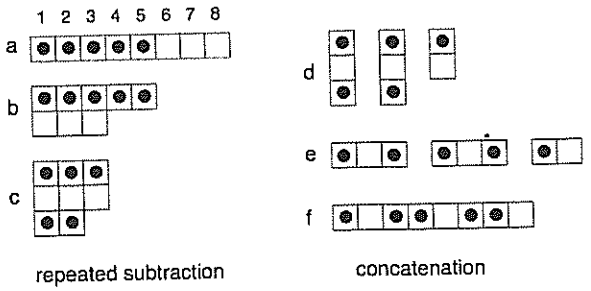

FIGURE 21.3 Generation of the Cuban *cinquillo* timeline.

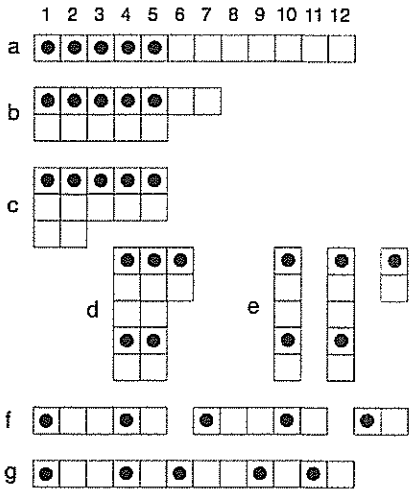

FIGURE 21.4 Generation of an Aka Pygmie timeline.

If we apply this algorithm with the numbers 5 and 12, illustrated in Figure 21.4, we obtain the rhythm E(5,12) = [3-2-3-2-2], which is a timeline played on a metal bell by the Aka Pygmies of Central Africa.[6]

Applying the algorithm to the pair of numbers (7, 12), as shown in Figure 21.5, results in the rhythm E(7,12) = [2-1-2-2-1-2-2], a popular West African bell pattern used in Ghana and Guinea.

Substituting the pair of numbers (5, 16) into the algorithm, illustrated in Figure 21.6, yields the rhythm E(5,16) = [3-3-3-3-4], a popular rhythmic pattern used in modern electronic dance music (EDM), which is a rotation of the bossa-nova timeline.[7]

The reader may have noticed that the Euclidean tresillo rhythm E(3,8) and the Euclidean cinquillo rhythm E(5,8) have a special relation with each other, evident from their circular representations in Figure 21.7. The tresillo [3-3-2] is shown on the left diagram. The *complement* of the tresillo (which consists

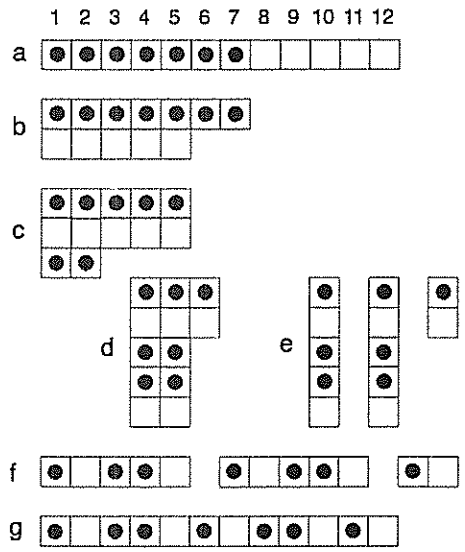

FIGURE 21.5 Generation of a ternary West African timeline.

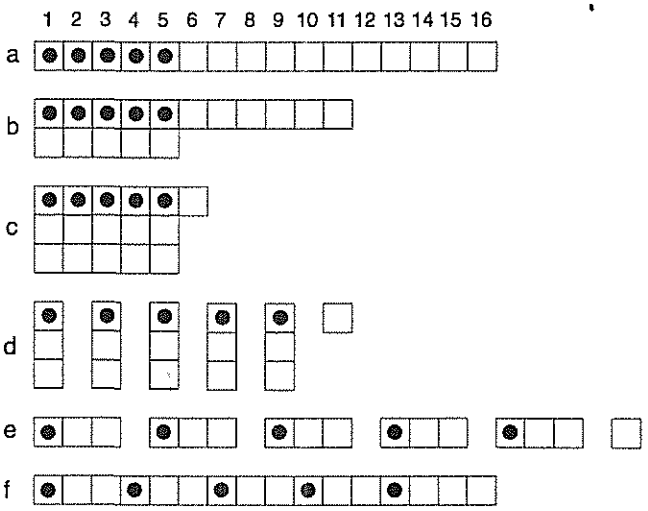

FIGURE 21.6 Generation of a binary West African timeline, which is also the signature rhythm of EDM.

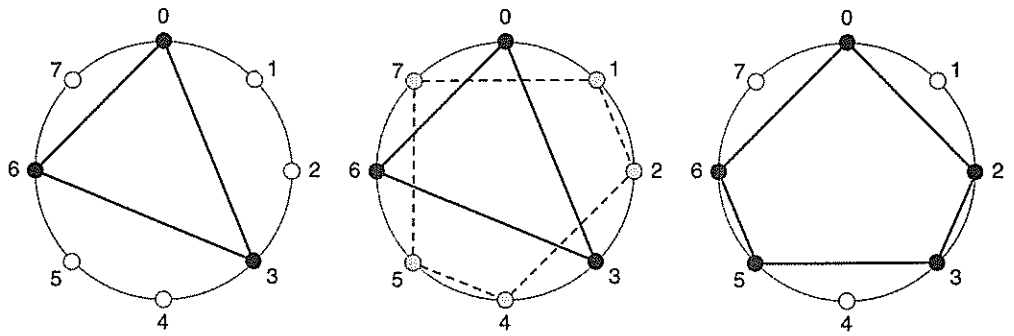

FIGURE 21.7 The tresillo (left), the complement of the tresillo in dashed lines and gray-filled circles (center), and the cinquillo (right).

of the silent pulses) is shown in dashed lines and gray-filled circles, in the center diagram. If the complement of the tresillo is rotated clockwise by a duration of one pulse, one obtains the cinquillo rhythm on the right diagram. You may ask yourself if it is a coincidence that, for the Euclidean tresillo rhythm, its complementary rhythm is also a Euclidean rhythm? Or is this a more general property of Euclidean rhythms? Before we answer this question let us calculate the Euclidean rhythm obtained with 11 onsets and 16 pulses. Note that $11 = 16 - 5$, which corresponds to the number of silent pulses in the West African timeline of Figure 21.6.

The application of the Euclidean algorithm to the sequence of 11 onsets in 16 pulses, depicted in Figure 21.8, yields the Euclidean rhythm E(11,16) = [1-2-1-2-1-2-1-2-1-2-1], which is a rotation of the complementary rhythm of the West African timeline shown in Figure 21.9 (right). The Euclidean rhythm E(11,16) starts on pulse 14 in the rightmost diagram, where it is superimposed on the West African timeline. Therefore, the complement of E(5,16) is E(11,16). More generally, reflections and rotations of Euclidean rhythms are obviously also Euclidean. Furthermore, it was proved by Jack Douthett and Richard Krantz that the complement of a Euclidean rhythm is also Euclidean.[8] Complementary rhythms will be revisited in more detail in Chapter 25.

Scores of other Euclidean rhythms that are used in music throughout the world may be generated in this way by suitably picking the number n of pulses and the number k of onsets in a cycle. A list of some examples of Euclidean rhythms used in traditional music practice, for values of n and k, such that k does not divide evenly into n, are listed in the following.

E(2,3) = [x x .] = [1-2]

E(2,5) = [x . x . .] = [2-3]

E(2,7) = [x . . x . . .] = [3-4]

E(3,4) = [x x x .] = [1-1-2]

E(3,5) = [x . x . x] = [2-2-1]

E(3,7) = [x . x . x . .] = [2-2-3]

E(3,8) = [x . . x . . x .] = [3-3-2]

E(3,10) = [x . . x . . x . . .] = [3-3-4]

E(3,11) = [x . . . x . . . x . .] = [4-4-3]

E(3,14) = [x . . . . x . . . . x . . .] = [5-5-4]

E(4,5) = [x x x x .] = [1-1-1-2]

E(4,7) = [x . x . x . x] = [2-2-2-1]

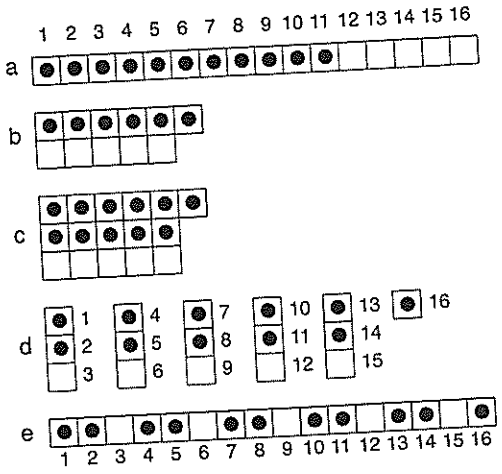

FIGURE 21.8 Generation of the complement of the binary West African timeline.

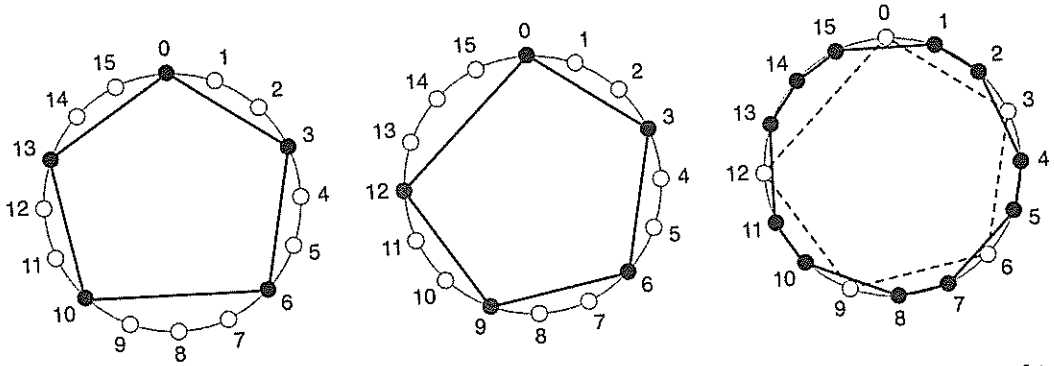

FIGURE 21.9 The bossa-nova (left), the West African timeline (center), and the complement of the West African timeline in black-filled circles (right).

E(4,9) = [x . x . x . x . .] = [2-2-2-3]

E(4,11) = [x . . x . . x . . x .] = [3-3-3-2]

E(4,15) = [x . . . x . . . x . . . x . .] = [4-4-4-3]

E(5,6) = [x x x x x .] = [1-1-1-1-2]

E(5,7) = [x . x x . x x] = [2-1-2-1-1]

E(5,8) = [x . x x . x x .] = [2-1-2-1-2]

E(5,9) = [x . x . x . x . x] = [2-2-2-2-1]

E(5,11) = [x . x . x . x . x . .] = [2-2-2-2-3]

E(5,12) = [x . . x . x . . x . x .] = [3-2-3-2-2]

E(5,13) = [x . . x . x . . x . x . .] = [3-2-3-2-3]

E(5,16) = [x . . x . . x . . x . . x . . .] = [3-3-3-3-4]

E(6,7) = [x x x x x x .] = [1-1-1-1-1-2]

E(6,13) = [x . x . x . x . x . x . .] = [2-2-2-2-2-3]

E(7,8) = [x x x x x x x .] = [1-1-1-1-1-1-2]

E(7,9) = [x . x x x . x x x] = [2-1-1-2-1-1-1]

E(7,10) = [x . x x . x x . x x] = [2-1-2-1-2-1-1]

E(7,12) = [x . x x . x . x x . x .] = [2-1-2-2-1-2-2]

E(7,15) = [x . x . x . x . x . x . x . .] = [2-2-2-2-2-2-3]

E(7,16) = [x . . x . x . x . . x . x . x .] = [3-2-2-3-2-2-2]

E(7,17) = [x . . x . x . . x . x . . x . x .] = [3-2-3-2-3-2-2]

E(7,18) = [x . . x . x . . x . x . . x . x . .] = [3-2-3-2-3-2-3]

E(8,17) = [x . x . x . x . x . x . x . .] = [2-2-2-2-2-2-2-3]

E(8,19) = [x . . x . x . x . . x . x . x . . x .] = [3-2-2-3-2-2-3-2]

E(9,13) = [x . x x . x x . x x . x x] = [2-1-2-1-2-1-2-1-1]

E(9,14) = [x . x x . x x . x x . x x .] = [2-1-2-1-2-1-2-1-2]

E(9,16) = [x . x x . x . x . x x . x . x .] = [2-1-2-2-2-1-2-2-2]

E(9,20) = [x . . x . x . x . x . . x . x . x . x .] = [3-2-2-2-3-2-2-2-2]

E(9,22) = [x . . x . x . . x . x . . x . x . . x . x .] = [3-2-3-2-3-2-3-2-2]

E(9,23) = [x . . x . x . . x . x . . x . x . . x . x . .] = [3-2-3-2-3-2-3-2-3]

E(11,12) = [x x x x x x x x x x x .] = [1-1-1-1-1-1-1-1-1-1-2]

E(11,20) = [x . x x . x . x . x x x . x . x . x .] = [2-1-2-2-2-2-1-2-2-2-2]

E(11,24) = [x . . x . x . x . x . . x . x . x . x . x .] = [3-2-2-2-2-3-2-2-2-2-2]

E(13,24) = [x . x x . x . x . x . x x . x . x . x . x .] = [2-1-2-2-2-2-2-1-2-2-2-2-2]

E(15,34) = [x . . x . x . x . x . . x . x . x . x . . x . x . x . x . . x . x .] = [3-2-2-2-3-2-2-2-3-2-2-2-3-2-2]

The durational patterns in the earlier list should be viewed more generally as necklaces and bracelets rather than rhythms, since in many instances, rotations and/or reflections of these interonset intervals (IOI) patterns yield other rhythms that are also used in traditional music around the globe. For example, the rhythm E(2,3) = [x x .] when started on the second onset becomes [x . x], which is a rhythm of a *Drum Dance* song of the Slavey Indians of Northern Canada,[9] as well as the hallmark rhythm of the *Lenjengo* recreational dance of the Mandinka people of West Africa.[10] Starting the rhythm E(3,4) = [x x x .] on the third onset yields [x . x x], which is the Arabic rhythm *wahdah sāyirah*.[11] Starting the rhythm E(3,7) = [x . x . x . .] on the third onset yields [x . . x . x .], which is the meter of the *aksak Bešli i čaj tele*.[12] Similarly, starting E(5,16) = [x . . x . . x . . x . . x . . .] = (33334) on the third onset yields the bossa-nova clave [3-3-4-3-3].[13] Furthermore, the patterns in this list are also expressed in their shortest form. Linear stretching of these rhythms will produce other rhythms. For example, when E(2,3) = [x x .] = [1-2] is multiplied by two it becomes [x . x . . .] = [2-4], a variant of the Mexican *son* rhythm.[14]

Euclidean rhythms are closely related to a similar concept studied in theoretical computer science: *Euclidean strings*.[15] Let $V = (v_0, v_1, ..., v_{n-1})$ denote a string of integers such as an interval vector of a rhythm. A string $V = (v_0, v_1, ..., v_{n-1})$ is a *Euclidean string* if increasing the duration v_0 by one, and decreasing the duration v_{n-1} by one, yields a new string that is a rotation of V. For example, if the operation is applied to the Euclidean rhythm E(4,9) = [2-2-2-3], one obtains [3-2-2-2], and since this is a rotation of [2-2-2-3], it follows that E(4,9) is a Euclidean string.[16] On the other hand, the rhythm [3-3-2-2-2] is not a Euclidean string because [4-3-2-2-1] is not a rotation of [3-3-2-2-2].

The reader may have noticed that the Euclidean rhythms are composed of IOIs of two sizes. For example, E(3,8) = [3-3-2], E(3,11) = [4-4-3], E(3,14) = [5-5-4], and E(5,12) = [3-2-3-2-2]. Furthermore, whatever the two IOI values are, they differ by exactly one pulse. However, there

exist rhythm timelines that consist of more than two IOI values, such as the Pygmy BaYaka rhythm [2-2-2-1-2-3], the Pygmy Mbuti rhythm [6-4-2-4], and of course, the ubiquitous *clave son* [3-3-4-2-4]. Furthermore, there exist rhythm timelines that, like Euclidean rhythms, consist of precisely two IOI values, such that these values differ by more than one pulse, such as the Bushmen San timelines [2-4-4-2-4], [6-6-4], and [4-6-4-6].[17] Rhythms that consist of IOIs of precisely two values, such that the IOIs are maximally evenly distributed are called *well-formed* rhythms.[18] The Euclidean algorithm that generates Euclidean rhythms when applied to sequences of two-valued pulse symbols can also be used to generate *well-formed* rhythms by merely substituting the two-valued pulse symbols with two-valued IOI symbols. For example, assume we wish to generate a well-formed rhythm with three IOIs of four pulses and two IOIs of two pulses, and refer to Figure 21.10. We begin in row, Figure 21.10a, by listing the two groups of IOI symbols, as we did with the onsets and silent pulses (rests) for generating Euclidean rhythms. Repeated subtraction until one column is left yields row, Figure 21.10b. Reading, Figure 21.10b, from top to bottom and left to right yields, Figure 21.10c, which when concatenated yields the well-formed IOI pattern [4-2-4-2-4], which in turn yields the well-formed (non-Euclidean) rhythm in box notation in row, Figure 21.10e. Note that this rhythm is a rotation of the 16-pulse Bushmen San timeline [2-4-4-2-4].

To conclude this chapter, it should be noted that the Euclidean algorithm has also been applied to music in a completely different context. Viggo Brun used it in the construction of stringed musical instruments, in which there are constraints on the lengths of the strings as well as on the ratios of these lengths.[19]

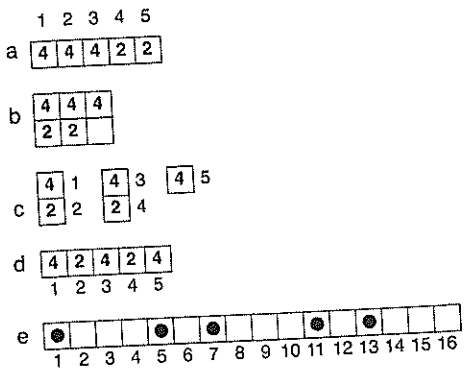

FIGURE 21.10 Illustration of how the Euclidean algorithm applied to IOIs can be used to generate the *well-formed* rhythm [4-2-4-2-4].

NOTES

1 Beckman, P., (1971).

2 Toussaint, G. T., (1993), traces the history of the second proposition of Book I of the *Elements*, which in effect states that any problem that can be solved with a straight edge and the *modern* compass can also be calculated with a straight edge and the *collapsing* compass. The distinction between the two compasses is that with the modern compass one is permitted to transfer a distance from one location on the paper to another, whereas this is not allowed with the collapsing compass. Not surprisingly, algorithms that utilize the collapsing compass require more steps than those that employ the modern compass.

3 Bach, E. & Shallit, J., (1996), p. 67.

4 Sacks, O., (1998).

5 Stewart, J., (2010), p. 173.

6 Chemillier, M., (2002), p. 175. The Aka Pygmies of Central Africa use several additional rhythms with a similar pattern consisting of two intervals of duration three followed by two groups of elements of duration two, such that the cardinality of the two groups differs by one. Such rhythms include [3-2-2-3-2-2-2] and [3-2-2-2-2-3-2-2-2-2-2].

7 Butler, M. J., (2001).

8 Euclidean rhythms are *maximally even*. Douthett, J. & Krantz, R. J., (2008), p. 205 proved that the complement of a maximally even rhythm is maximally even, thereby establishing the result for Euclidean rhythms. See also Amiot, E., (2007), p. 12, for an alternate proof of this property.

9 Asch, M. I., (1975), p. 249.

10 Knight, R., (1974), p. 28.

11 Touma, H. H., (1996), p. 50.

12 Goldberg, D., (2015).

13 Butler, M. J., (2006), p. 147, points out that [3-3-3-3-4] is a rhythm often used in EDM.

14 Stanford, E. T., (1972), p. 79.

15 Ellis, J., Ruskey, F., Sawada, J., & Simpson, J., (2003). Euclidean strings are a topic that falls under the more general *theory of words*. Domínguez, M., Clampitt, D., & Noll, T., (2009), provide a translation bridge between the theory of words and music theory.

16 See Toussaint, G. T., (2005c), for a more detailed comparison of Euclidean rhythms with Euclidean strings in the context of Balkan *aksak* rhythms and sub-Saharan African timelines.

17 Poole, A., (2018).

18 Milne, A. J., Herff, S. A., Bulger, D., Sethares, W. A., & Dean, R., (2016). XronoMorph: Algorithmic generation of perfectly balanced and well-formed rhythms. In *Proceedings of the 2016 International Conference on New Interfaces for Musical Expression*. Brisbane, Australia.

19 Brun, V., (1964), p. 128.

Visualization and Representation of Rhythms

In this book, I have up to this point used predominantly three notation systems that are most convenient for the types of analyses undertaken: the box notation (in several variations), the convex polygon notation, and the interonset interval (IOI) vector notation (numerical durational patterns). The first two approaches are geometric and emphasize visualization. The third method indicates duration with numbers. Another noteworthy numerical system is *gongche* notation, the traditional Chinese system that uses numbers to indicate pitches, and dots and lines for rhythm.[1] The musical information and the notation systems that encode this information are interdependent. They have their unique advantages and drawbacks, and different applications may benefit more from notation systems that are tailored to them.[2] Music performers, ethnomusicologists, and music psychologists may also benefit more from notation systems that are tailored to their particular needs.[3] In this chapter several additional notation systems are reviewed, and the contexts in which they are used are indicated. Standard Western music notation is notably left out of this discussion because its descriptions are ubiquitous.

ALTERNATING-HANDS BOX NOTATION

In Chapter 35, a technique using alternating hands was described for generating toggle rhythms. The technique is also ideal for teaching and learning hand drumming. Recall that it consists of continuously, and gently, striking the drum by alternating with the right and left hand, much like walking, making sure that all the durations between two consecutive strikes are equal, and that all the sounds made are identical to each other, much like a metronome.[4] The box notation system can be modified so that it provides a clearer visualization of the alternating-hands process and that it is easy to read while practicing the technique, as illustrated in Figure 35.1. This notation also helps the student understand and remember the structure of the rhythms more easily. In addition, it helps the student acquire coordination, left–right independence, and timing precision, by embodying a metronomic sense of pulse that is essential for mastering rhythmic performance.

The idea is simple: use two side-by-side sequences of boxes, one for each hand, and rotate them to a vertical position so that the left and right hands play the left and right columns, respectively. In Figure 35.1 time flows from the bottom to the top. On the left is the *clave son*, and on the right the clave rumba. The differences between the two rhythms are highlighted by the onsets played by the left hand. The *clave son* contains only one left-hand onset at pulse three, whereas the clave rumba contains an additional left-hand onset at pulse seven. In order to develop proper left–right independence, playing with the reversal of the roles of the left and right hands should also be mastered.

SPECTRAL NOTATION

Consider the IOI durations of the *clave son* [3-3-4-2-4] and plot these numbers, in the order in which they occur, as heights of bars in a bar graph, such as that illustrated in Figure 35.2 (left). This type of notation has been used by researchers in the linguistics field interested in the

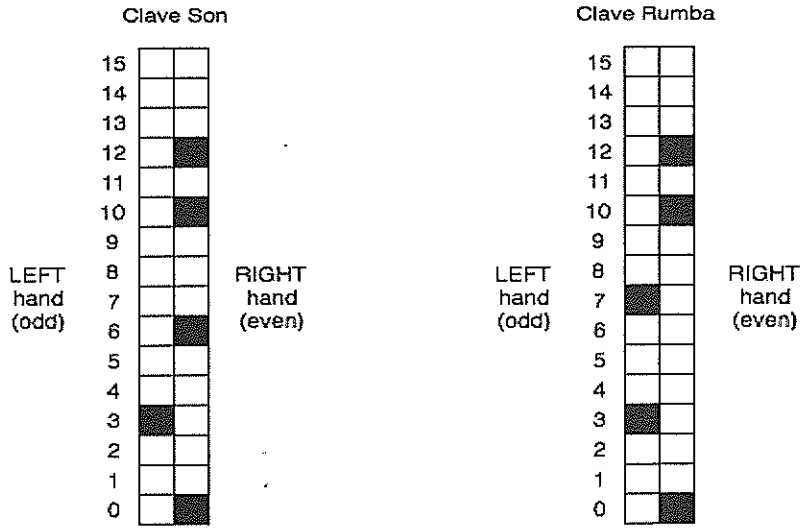

FIGURE 35.1 The *alternating-hands* box notation.

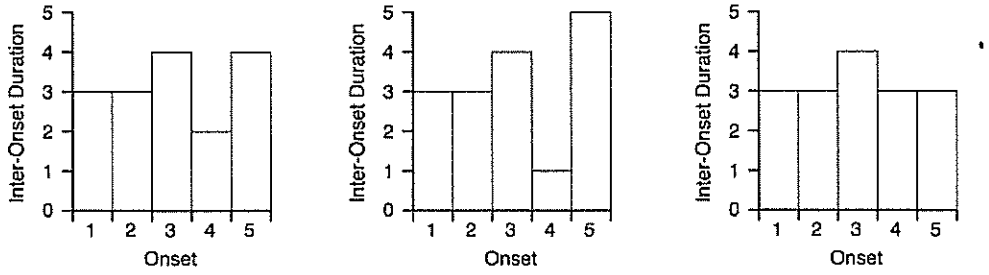

FIGURE 35.2 From left to right, respectively, the *son*, *soukous*, and *bossa-nova* timelines in spectral notation.

analysis of speech rhythms. This notation provides a compact view of the *spectrum* of the IOIs in the order in which they appear in time, and it accentuates the irregularity (or regularity) of the rhythm. Hence, we call it spectral notation. In Figure 35.2 it may be perceived quite compellingly that the bossa-nova (right) is more regular (uniform) than the soukous (middle).

Any rhythm notation system suggests a variety of new methods for measuring the distance (dissimilarity) between rhythms, and spectral notation is no exception. A natural way to measure distance in this case is by overlaying one spectrum over the other and calculating the area of the region in between the two curves, as shown in Figure 35.3.

On the left, the spectra of the *clave son* and bossa-nova are superimposed over each other, and the area difference between the two curves, highlighted in dark gray, is 2. On the right, the bossa-nova spectrum is superimposed over the soukous spectrum to reveal an area between the curves equal to 4. Thus, we conclude that the bossa-nova is more similar to the son than to the soukous.

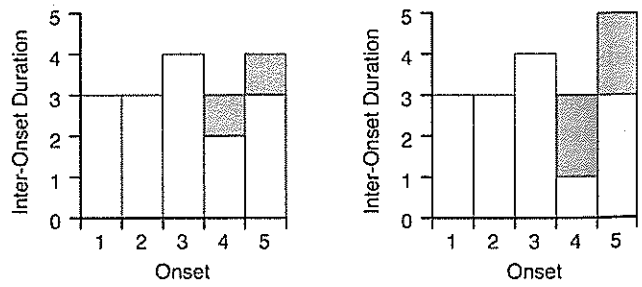

FIGURE 35.3 The area difference between the spectra of the *son* and the *bossa-nova* (left), and between the spectra of the *bossa-nova* and the *soukous* (right).

TEDAS NOTATION

A disadvantage of the spectral notation elucidated in Figure 35.3 is that the veracity of the relative time durations of the IOIs along the time axis is lost because these

intervals are displayed in the vertical direction. In an attempt to recover this valuable lost visual information, while at the same time maintaining some of the advantages of the spectral notation, in 1987 Kjell Gustafson, a researcher at the Phonetics Laboratory of the University of Oxford interested in displaying speech rhythm, proposed an original and simple method that places time on both the vertical and horizontal axes.[5] Since an element that displays the durations along two orthogonal directions determines a square, Gustafson called his notation TEDAS notation, an acronym for *Time Elements Displayed as Squares*. Figure 35.4 shows (top to bottom) the son, soukous, and bossa-nova timelines in TEDAS notation.

The TEDAS notation also suggests measuring the distance between rhythms by the area difference of their graphs.[6] In Figure 35.5 (left), the TEDAS graphs of the son and bossa-nova superimposed over each other yield an area difference between the two curves, highlighted in dark gray, equal to 6. On the right, the TEDAS graph of the son superimposed over the TEDAS graph of the soukous yields an area between the curves equal to 8. Thus, by this measure, we may conclude that the son is more similar to the bossa-nova than to the soukous. By representing the IOI durations as squares of the durations, the TEDAS notation places greater emphasis on longer IOIs, since two-dimensional area grows as the square of the one-dimensional duration. How the application of such a weighting scheme of the IOIs to the design of similarity measures affects the predictability of human judgments is still an open problem.

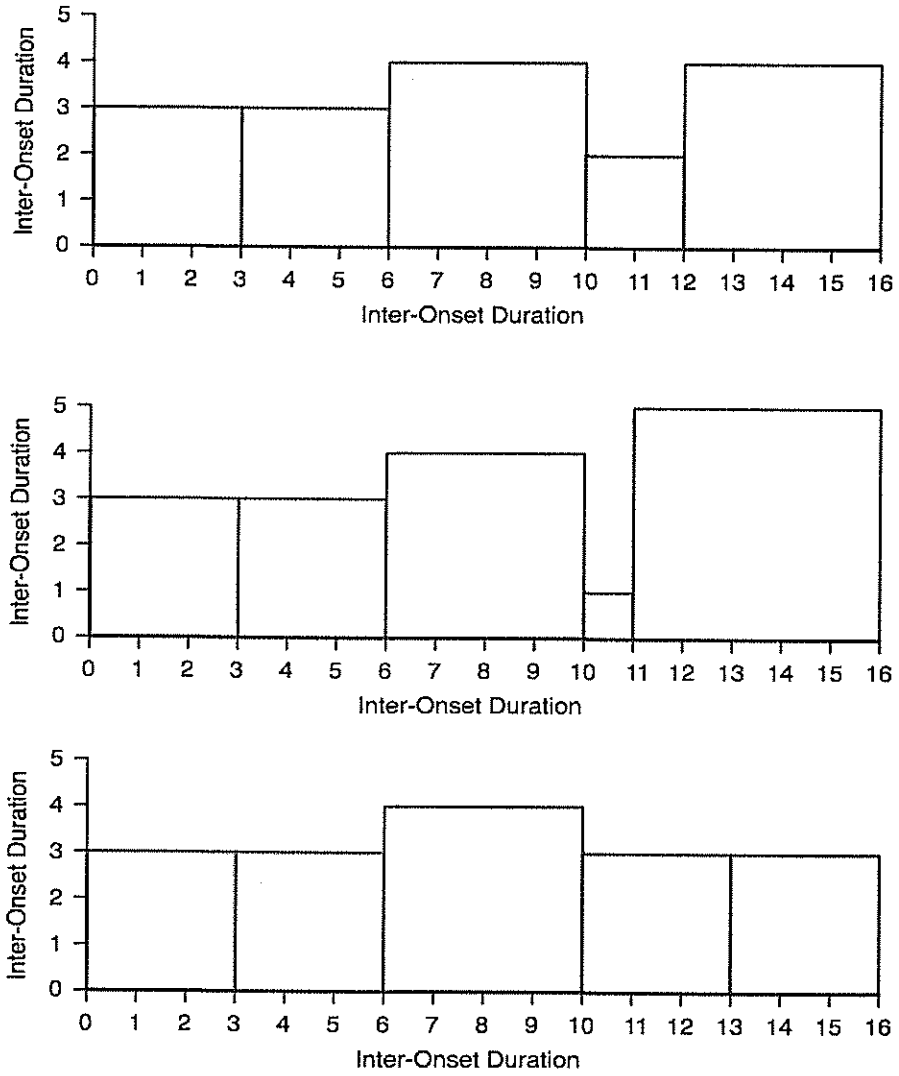

FIGURE 35.4 The *son*, *soukous*, and *bossa-nova* timelines in TEDAS notation.

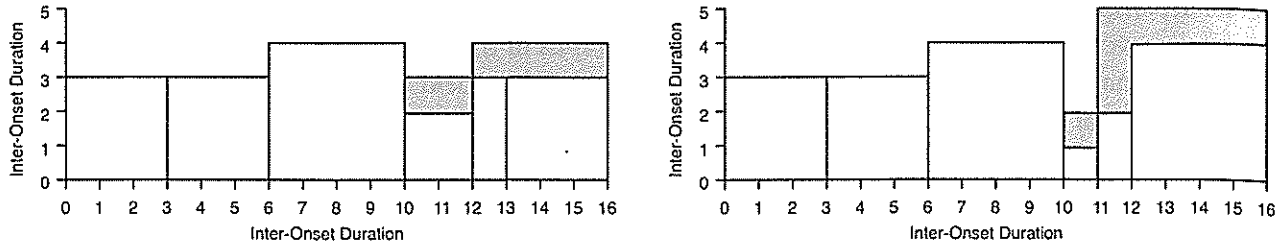

FIGURE 35.5 The area difference between the *son* and the *bossa-nova* (left), and between the *son* and the *soukous* (right).

CHRONOTONIC NOTATION

A variant of the TEDAS notation was later discovered by the music psychologist Ludger Hofmann-Engl who christened it *chronotonic* notation. In this notation, every onset of duration k pulses receives k *atoms* (pulses) of height k. The sequence of atoms of a rhythm connected by line segments between adjacent atoms determines a *chonotonic chain*. Figure 35.6 illustrates the *chronotonic chain* obtained for the *clave son*.

Hofmann-Engl also defined a measure of rhythm similarity based on a function of the difference between two chronotonic chains. Furthermore, it was shown by means of psychological experiments that the measure exhibits considerable agreement with human perception of rhythmic similarity.[7] How this measure compares with other more well-known measures, such as the edit distance, is yet to be determined.

PHASE SPACE PLOTS

A phase space plot consists of a mapping of adjacent IOI durations onto a two-dimensional coordinate space (the Euclidean plane), such that the first two IOI durations determine a point $p_1(x,y)$ with x-coordinate equal to the first IOI duration, and y-coordinate equal to the second IOI duration. This point $p_1(x,y)$ is connected with a straight edge to a point $p_2(x,y)$ that has x-coordinate equal to the second IOI duration and y-coordinate equal to the third IOI duration, and so forth.[8] In general, if the rhythm has n onsets (attacks), the phase space plot has n points $p_1(x,y)$, $p_2(x,y)$, ..., $p_n(x,y)$ corresponding to n pairs of adjacent IOI durations, such that $p_i(x,y)$ has an x-coordinate equal to the duration of IOI_i and a y-coordinate equal to the duration of IOI_{i+1}, for $i = 1, 2, \ldots, n$. Since the rhythms are cyclic, IOI_{n+1} corresponds to the IOI duration between the last and first onsets. Figure 35.7 shows the phase space plots of the six distinguished timelines. Points that lie on the diagonal dashed line (called the *isotropy line*) correspond to pairs of adjacent IOIs that have the same duration. Note that the plot of the rumba has no vertex on the isotropy line since it does not contain any pair of adjacent IOIs of the same duration. The plots are general polygons (phase space polygons also called embedding graphs[9]) whose vertices and edges may fall on top of each other (self-intersect), as is the case with five of these rhythms. These six phase space polygons may be classified into two classes. The shiko, son, and bossa-nova fall in one class, and are distinguished from the other three by the property that their phase space polygons have reflection symmetry about the isotropy line. Furthermore, the *clave son* is unique among the six by virtue of the property that it is the only rhythm whose phase space polygon

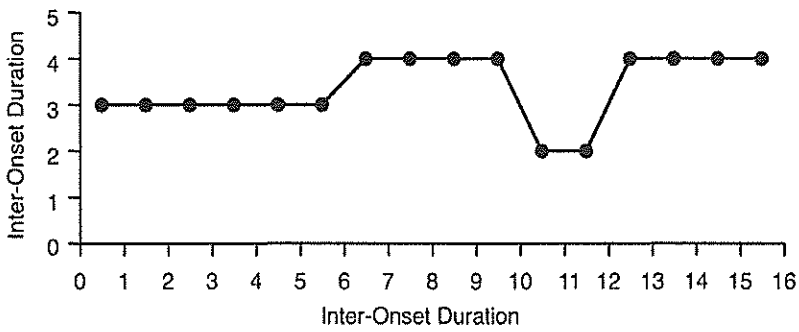

FIGURE 35.6 The chronotonic chain of the *clave son*.

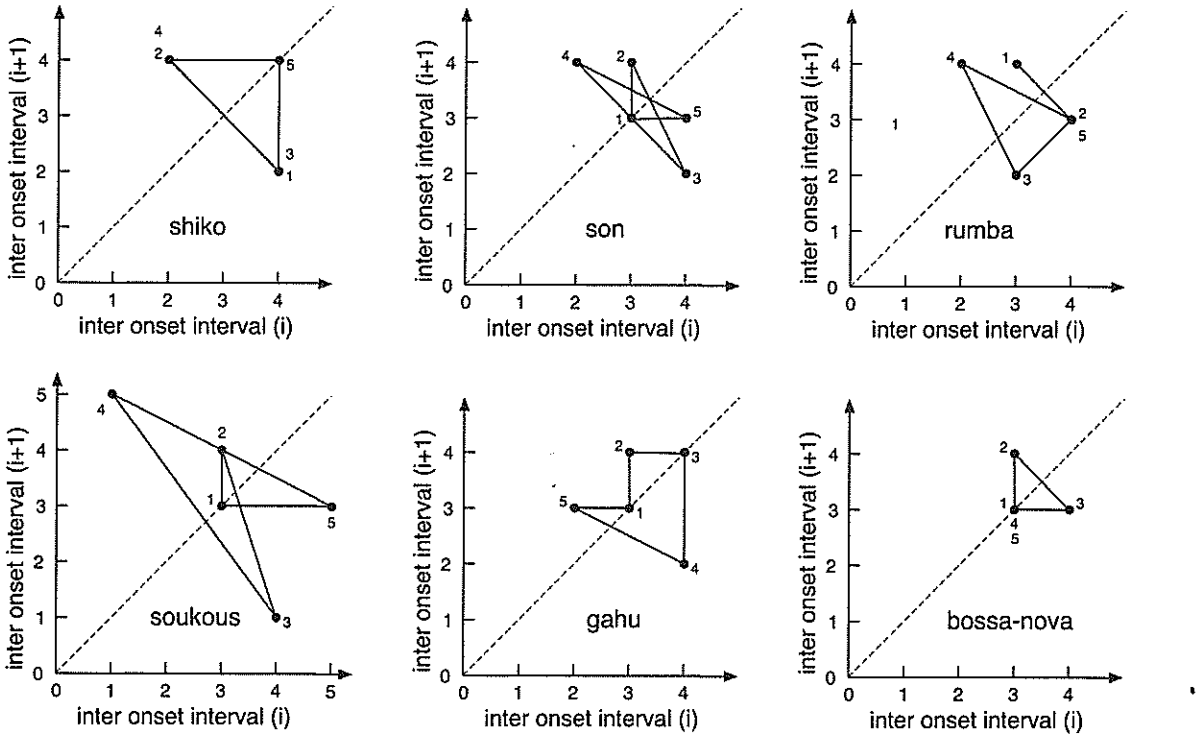

FIGURE 35.7 The phase space plots (polygons) of the six distinguished timelines.

has reflection symmetry and no two vertices lie on top of each other. The gahu is also uniquely distinguishable from the other five, since it is the only rhythm that has a phase space plot that is a *simple* polygon. A polygon is simple provided that all its vertices are unique, and it has no self-intersections.[10] Only the gahu has a phase space plot composed of a simple polygon.

Phase space plots provide a tool for artistic and analytical exploration of rhythmic structures. In the acoustic domain, they have been applied to audio-based music visualization for music structure analysis, with the goal of facilitating users to browse through music collections, in the context of music information retrieval.[11] The application of phase space plots to the analysis of symbolically represented rhythms is still an area in its infancy waiting to be mined.

Any representation of rhythms suggests methods to measure rhythm similarity, and phase space plots are no exception. Two phase space plots may be compared quantitatively by measuring their musically relevant geometric features and then calculating the distance between the resulting feature vectors. To illustrate the usefulness of phase space plots and the measurement of their similarity for the case of rhythm timelines, let us return to the problem of binarization of the ternary fume–fume timeline [2-2-3-2-3] by means of the natural (proximity Gestalt inspired) algorithm that snaps the onsets of the fume–fume in a 12-pulse span to their nearest pulses in an overlaid 16-pulse span. This problem, left unsettled in Chapter 12, will be resolved here geometrically. The nearest pulse snapping algorithm generated three different possible binarizations of [2-2-3-2-3], namely [3-2-4-3-4], [3-3-4-2-4], and [2-3-4-3-4], raising the question of explaining the claims made by ethnomusicologist Rolando Pérez-Fernández that the *clave son* [3-3-4-2-4] is the "correct" one.[12] In Chapter 12 it was attempted to resolve this problem by calculating the total quantization errors obtained with the global Minkowski metrics, for its three binarizations, for the cases of the Manhattan, Euclidean, and Maximum metrics. The best result (obtained with the Maximum metric) resulted in a tie that was broken by invoking the psychological Gestalt spatial theory of rhythmic resolution.[13] In more concrete terms, for our special case, the fume–fume begins with two IOIs of the same duration [2-2], and the only binarization that also starts with two IOIs of equal duration, the *clave son* with [3-3]. However, it is possible to resolve the problem with purely geometrical global similarity measures using the phase space plots, as shown later using two different approaches.

Two musically relevant geometric features of the plots are (1) the number of polygon vertices that lie on the isochrony line and (2) the presence or absence of reflection symmetry of the polygon about the isochrony line. The fume–fume polygon has one vertex on the isochrony line as well as reflection symmetry with respect to this line. By contrast, the phase space polygons of the binarizations [3-2-4-3-4] and [2-3-4-3-4] do not share either of these properties, whereas the polygon corresponding to the *clave son* enjoys both properties. By this comparison metric, it follows that the *clave son* is the binarization most similar to the fume–fume (Figure 35.8).

For the second geometric resolution of the binarization problem, we need some additional terminology and definitions. The similarity between two phase space polygons may also be measured using the areas of their *convex hulls*. A polygon is *convex* if the line segment connecting every pair of points that lie in the polygon also lies completely in the polygon. Figure 35.9 (left) illustrates a convex polygon, where x and y represent any two points in the polygon. The polygon on the right in this figure is not convex because there exists a pair of points x and y such that the line segment connecting them passes through the exterior of the polygon. The area of the convex hull of a set in the Euler lattice has been used previously as a feature for characterizing chords and scales in terms of their preference. It turns out that this feature is also helpful in the rhythm domain.

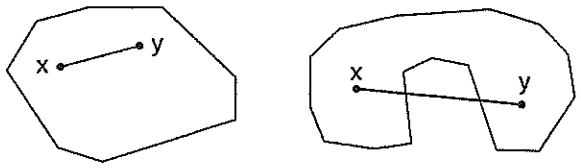

FIGURE 35.9 A convex polygon (left) and a nonconvex polygon (right).

A polygon is said to be *star-shaped* if there exists a point x in the polygon such that for every point y in the polygon the line segment connecting x and y also lies completely in the polygon. Intuitively, if the star-shaped polygon is considered to be the floor plan of an art gallery, then one guard suitably located can see the entire gallery from that spot.[14] The polygon in Figure 35.10 (left) shows one such location x from which the entire polygon is visible. Recall that a polygon is called *simple*

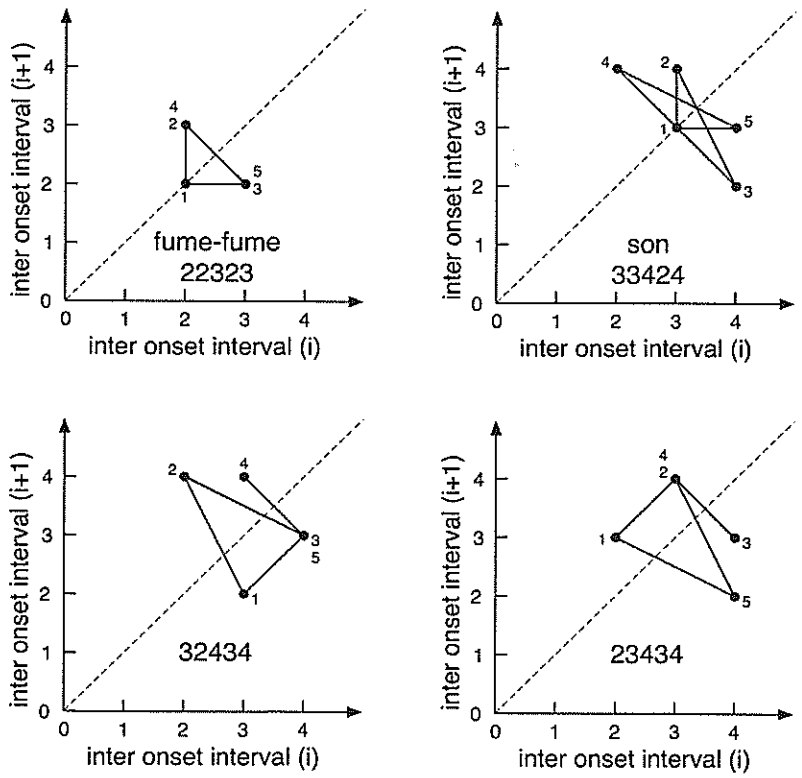

FIGURE 35.8 The phase space plots of the ternary fume–fume and its three binarizations resulting from the nearest onset snapping rule.

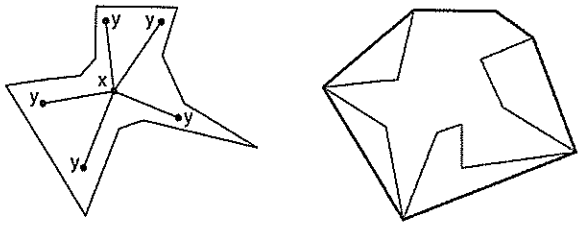

FIGURE 35.10 A star-shaped polygon (left) and the convex hull of a simple polygon (right).

provided that its boundary does not intersect itself. In Figure 35.7 the only phase space polygon that is simple is the one that represents the gahu timeline. All the other five polygons are self-intersecting. Furthermore, the gahu polygon is star-shaped, since it is entirely visible from its vertex labeled number 1. The *convex hull* of a polygon is the convex set of minimum area that encloses it. Figure 35.10 (right) shows a polygon (shaded) and its convex hull (bold lines). Intuitively, if an elastic band is wrapped around the polygon, it will take on the shape of a convex polygon that is precisely the convex hull of the polygon.[15] These notions of convexity and star-shapedness (also called star-convex) have been successfully applied to the analysis of spaces of chords, scales, and harmony in the pitch domain.[16] Indeed, when the intervals of traditional musical scales are represented on an Euler lattice, all of them form star-shaped structures.[17] This property may thus qualify as a universal in music and provides inspiration to search for similar rhythmic universals by means of geometric methods.

With this additional terminology, let us return to the binarization problem of the fume–fume [2-2-3-2-3]. Figure 35.11 shows the convex hulls (shaded) of the phase space polygons for the fume–fume as well as its three binarization candidates. The areas of their convex hulls are: 0.5 for the fume–fume, 1.5 for the *clave son*, and 2.0 for the two additional binarizations [3-2-4-3-4] and [2-3-4-3-4]. Therefore, by comparing the magnitude of the areas, it follows that the *clave son* is again the binarization most similar to the fume–fume. Whether phase space plots of rhythms will be useful for measuring rhythm similarity in more general settings is a research problem yet to be explored.

TANGLE DIAGRAMS

The visualization techniques described in the preceding are useful for all types of rhythms. In addition, there are some specific visualization techniques

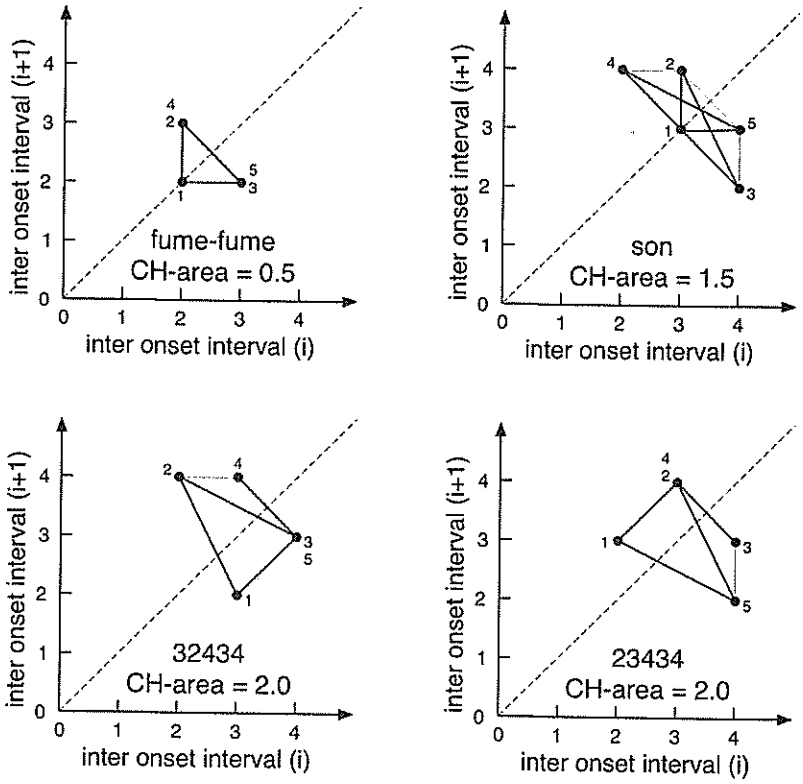

FIGURE 35.11 The convex hulls (shaded) of the phase space plots of the ternary fume–fume and its three binarizations.

that emerge from the structure of restricted classes of rhythms. The application of *tangle theory*, a branch of topology closely related to knot theory, to the visualization of Euclidean rhythms is a case in point.[18] We have seen in Chapter 21 titled Euclidean rhythms, that given two numbers k and n, where n is the number of pulses and k is the number of onsets, the Euclidean algorithm generates the Euclidean rhythm $E(k,n)$. The Euclidean algorithm may also be used to generate the continued fraction of the rational number k/n. Furthermore, there is a one-to-one correspondence between a continued fraction of a rational number and a tangle.[19] A *tangle diagram* consists of a circle with two vertices near the top and two near the bottom. The top vertices are connected to the bottom vertices with arcs that may intertwine with each other. Figure 35.12 shows the tangle diagrams for the tresillo Euclidean rhythm [2-1-2-1-2] (left), and the 13-pulse rhythm [3-2-3-2-3] (right). The tangle diagram on the right is clearly visually more complex than the one on the left, suggesting that the 13-pulse Euclidean rhythm is more complex than the cinquillo. There is thus the possibility that there exists a correlation between the visual complexity of the tangle diagram of a rhythm, and the aural perceptual complexity of the rhythm. However, this question has not been investigated. How useful tangle diagrams will be for the analysis of rhythm in the future only time will tell.

In closing this chapter, it should be noted that the new technologies being developed around the application of computer software and hardware, for a variety of purposes such as notation, analysis, education, games, and composition, have spurred an explosion of new visualization techniques that explore graph techniques in two dimensions (such as tree languages[20]), and three-dimensional spaces.[21] There is now an annual conference called TENOR[22] (International Conference on Technologies for Music Notation and Representation) that explores this exploding field of research.

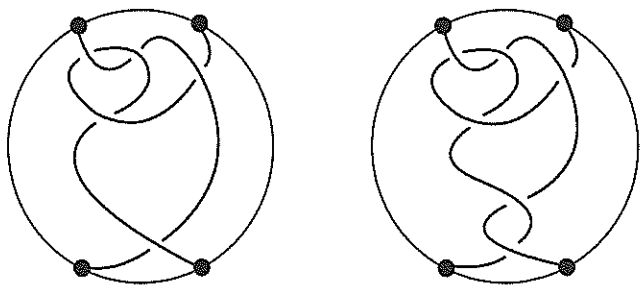

FIGURE 35.12 The *tangle* diagrams corresponding to the Euclidean cinquillo rhythm (left) and the 13-pulse rhythm [3-2-3-2-3] (right).

NOTES

1 Lau, F., (2008). p. 52.

2 Cohen, D. & Katz, R., (1979). Ellingson, T., (1992), focuses on notation systems developed in several cultures. See also Ellingson, T., (1992) and Kaufman Shelemay, K., (2000). Koetting, J. & Knight, R., (1986), p. 60, find that box notation is convenient for their "fastest pulse analysis" of rhythm. Brinkman, A. R., (1986), describes a binomial notation system for pitch that codes additional information. Benadon, F., (2009a), provides tools for notating microtiming in jazz while minimizing the complexity of notation. For a comparison of several mathematical notation systems, see Liu, Y. & Toussaint, G. T., (2010a).

3 For instance, Perkins, D. N. & Howard, V. A., (1976), p. 76, propose a "psychological" notation system that visually reflects the "clustering" or figural perceptual grouping of the attack points of a rhythm.

4 Konaté, F. & Ott, T., (2000), p. 20. With this technique, also called "hand-by-hand" drumming, the performer playing a beat pattern also feels all the pulses in between the beats, which aids the acquisition of a metronomic precision.

5 Gustafson, K., (1987, 1988).

6 The application of the difference in area between two curves has also been applied to geometric measures of melodic similarity, where the melody curves represent pitch as a function of time. See ÓMaidín, D., (1998), Aloupis, G., Fevens, T., Langerman, S., Matsui, T., Mesa, A., Nuñez, Y., Rappaport, D., & Toussaint, G., (2006), and Lubiw, A. & Tanur, L., (2004).

7 Hofmann-Engl, L., (2002).

8 Ravignani, A., (2017). See also Ravignani, A. & Norton, P., (2017), for additional references and applications of the phase space plots to the analytic exploration of music.

9 Monro, G. & Pressing, J., (1998).

10 Toussaint, G. T., (1991). See also Meisters, G. H., (1975), for additional interesting properties of simple polygons, and Grünbaum, B., (1998), for enumeration of a class of self-intersecting polygons.

11 Wu, H.-H. & Bello, J. P., (2010).

12 Pérez-Fernández, R. A., (1986) and Pérez Fernández, R. A., (2007).

13 See McLachlan, N., (2000), for his spatial theory of rhythmic resolution.

14 Avis, D. & Toussaint, G. T., (1981).

15 Toussaint, G. T., (1985).

16 See the papers by Honingh, A.K. & Bod, R., (2005), for a treatment of convexity and the well-formedness of musical objects, Honingh, A. K., (2006), for convexity

and compactness as models for the preferred intonation of chords, and Honingh, A. K., (2009), for finding automatic modulation using convex sets of notes.

17 Honingh, A. K., & Bod, R., (2011).

18 Kirk, J. & Nicholson, N., (2016).

19 Conway, J., (1970).

20 Jacquemard, F., Ycart, A., & Sakai, M., (2017).

21 See the online papers by Ham, J. J., (2017), for 3-D spatial drum notation, and by Kim-Boyle, D., (2017), for 3-D score notation systems.

22 The conference proceedings of TENOR may be found here: www.tenor-conference.org/proceedings.html.